ANTIMICROBIAL AGENTS AND CHEMOTHERAPY, Jan. 2005, p. 380–387 Vol. 49, No. 1
0066-4804/05/$08.00+0 doi:10.1128/AAC.49.1.380–387.2005

Real-Time In Vivo Bioluminescent Imaging for Evaluating the Efficacy of Antibiotics in a Rat *Staphylococcus aureus* Endocarditis Model

Yan Q. Xiong,[1,2]* Julie Willard,[1] Jagath L. Kadurugamuwa,[3] Jun Yu,[3] Kevin P. Francis,[3] and Arnold S. Bayer[1,2]

Department of Medicine, Division of Infectious Diseases, Harbor-UCLA Research and Education Institute, Torrance,[1] Geffen School of Medicine, University of California Los Angeles, Los Angeles,[2] and Xenogen Corp., Alameda,[3] California

Received 3 June 2004/Returned for modification 1 August 2004/Accepted 30 August 2004

Therapeutic options for invasive *Staphylococcus aureus* infections have become limited due to rising antimicrobial resistance, making relevant animal model testing of new candidate agents more crucial than ever. In the present studies, a rat model of aortic infective endocarditis (IE) caused by a bioluminescently engineered, biofilm-positive *S. aureus* strain was used to evaluate real-time antibiotic efficacy directly. This strain was vancomycin and cefazolin susceptible but gentamicin resistant. Bioluminescence was detected and quantified daily in antibiotic-treated and control animals with IE, using a highly sensitive in vivo imaging system (IVIS). Persistent and increasing cardiac bioluminescent signals (BLS) were observed in untreated animals. Three days of vancomycin therapy caused significant reductions in both cardiac BLS (>10-fold versus control) and *S. aureus* densities in cardiac vegetations ($P < 0.005$ versus control). However, 3 days after discontinuation of vancomycin therapy, a greater than threefold increase in cardiac BLS was observed, indicating relapsing IE (which was confirmed by quantitative culture). Cefazolin resulted in modest decreases in cardiac BLS and bacterial densities. These microbiologic and cardiac BLS differences during therapy correlated with a longer time-above-MIC for vancomycin (>12 h) than for cefazolin (~4 h). Gentamicin caused neither a reduction in cardiac *S. aureus* densities nor a reduction in BLS. There were significant correlations between cardiac BLS and *S. aureus* densities in vegetations in all treatment groups. These data suggest that bioluminescent imaging provides a substantial advance in the real-time monitoring of the efficacy of therapy of invasive *S. aureus* infections in live animals.

S. aureus infections represent a growing proportion of serious community-acquired and nosocomial infections, reflecting an expanding reservoir of at-risk patient populations (1–3, 14). Of note, an alarmingly high proportion of these infections are now being caused by multidrug-resistant strains, including fully vancomycin-resistant *S. aureus* strains (12, 19, 22). Therefore, new in vitro and in vivo technologies for screening novel antibiotics to prevent and treat these life-threatening infections are urgently needed.

Recently, a novel bioluminescent in vivo imaging system (IVIS) was developed which offers a sensitive and noninvasive technique for rapid, real-time monitoring of therapeutic efficacy; this technique has been demonstrated to work particularly well for monitoring bacterial infections in vivo (7, 9–11, 13, 21). IVIS consists of a highly sensitive charge-coupled device digital camera with accompanying advanced computer software for image data acquisition and analysis. This system captures photons of light emitted by bacteria that have been engineered to produce bioluminescence. Over the past several years, real-time bioluminescent imaging has been utilized to assess the therapeutic efficacy of various antibiotics, principally in models of acute and chronic soft tissue infection (9, 10). However, this technique has not yet been applied to endovascular infections such as infective endocarditis (IE).

* Corresponding author. Mailing address: Division of Infectious Diseases, St. John's Cardiovascular Research Center, Harbor-UCLA Research & Education Institute, 1124 W. Carson St., Torrance, CA 90502. Phone: (310) 222-3545. Fax: (310) 782-2016. E-mail: yxiong@ucla.edu.

The aims of the present study were threefold: (i) to develop and adapt a small-animal (rat) model of *S. aureus* IE for use with bioluminescent imaging, (ii) to utilize this model to monitor the progression of infection in live animals, and (iii) to assess the real-time efficacy of several conventional antistaphylococcal agents in this model.

This work was presented in part at the 104th General Meeting of American Society for Microbiology, abstr. D-122, New Orleans, La. 23 to 27, May 2004.

MATERIALS AND METHODS

Organism. *S. aureus* Xen29 was derived from the parental methicillin-susceptible *S. aureus* strain, ATCC 12600, as previously described (9–11). The Xen29 strain possesses a stable copy of a *Photohabdus luminescens*-modified, complete *lux* operon (*luxA* to *luxE*) at a single integration site in the bacterial chromosome (9–11) (Fig. 1). This strain is capable of producing both the luciferase enzyme and its substrate, thereby constitutively emitting a bioluminescent signal when the organism is metabolically active (9, 10). In addition, this strain forms biofilms on catheters (9, 10).

Antibiotics. Several antibiotics belonging to different classes and having different mechanisms of action were selected for these studies. Vancomycin, cefazolin, and gentamicin were purchased from American Pharmaceutical Partners Inc. (Los Angeles, Calif.), West-Ward Pharmaceutical Corp. (Eatontown, N.J.), and Phoenix Scientific Inc (St. Joseph, Mo.), respectively. These antibiotics were reconstituted in appropriate diluents, as recommended by the manufacturers.

Susceptibility testing. The MICs and MBCs of vancomcycin, cefazolin, and gentamicin were determined by a broth microdilution method at final inocula of either 10^5 or 10^7 CFU per ml in Mueller-Hinton broth (Difco, Detroit, Mich.) as specified in the guidelines of the National Committee for Clinical Laboratory Standards (17, 18). These inocula were chosen to encompass the range of bacterial densities generally found in experimental IE target lesions (25). The MIC and MBC were defined as the lowest concentration completely inhibiting growth and the lowest concentration killing ≥99.9% of the inoculum, respectively.

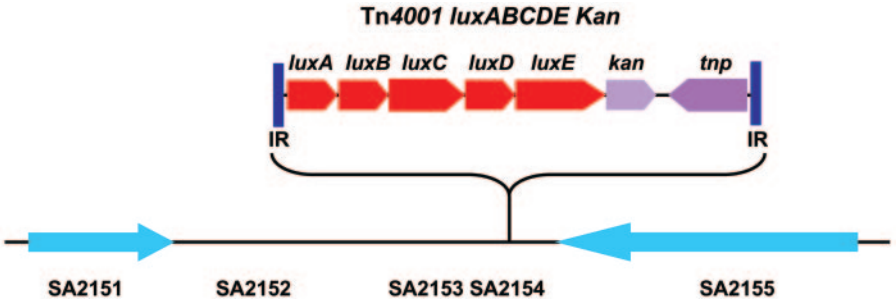

FIG. 1. *S. aureus* Xen29 genetic map. In strain Xen29, the transponson Tn*4001 luxABCDE kan* was inserted in the second open reading frame (SA2154) of a possible two-gene operon. The designations for the two open reading frames were SA2153 and SA2154. IR, inverted repeat.

In vitro detection of BLS. We evaluated the in vitro bioluminescence profile of *S. aureus* Xen29 in the presence and absence of polyethylene catheters (as used to induce rat IE [see below]). Briefly, the catheter was cut into ~3-cm segments, and each piece was sterilized with 70% ethanol and air dried. *S. aureus* Xen29 was cultured overnight in tryptic soy broth (TSB; Difco, Detroit, Mich.) supplemented with 0.25% glucose (TSBG) to optimize growth. The culture was diluted in fresh TSBG to reach a final inoculum of 10^7 CFU/ml; this suspension was then used to inoculate sterile six-well microtiter plates, with or without a sterile catheter segment. After 5 and 24 h of incubation at 37°C, bioluminescent signals (BLS) were monitored for 1 min by using the IVIS imaging system (Xenogen Corp., Alameda, Calif.) (see below for quantification details). As controls, catheters were prepared as above and placed in wells with media but without the bacterial inoculum.

Rat IE model. Sprague-Dawley female rats (250 to 300 g each) were obtained from Harlan Inc. (Indianapolis, Ind.). All animals were housed in the animal facility on-site, and all experimental procedures adhered to a protocol approved by the Institutional Animal Care and Use Committee. A well-characterized experimental rat IE model was used in the present studies, as previously described (6, 15). In brief, the animals were maintained in an anesthetized state with an isofluorane-oxygen gas mixture (1:1 ratio) during surgery. An indwelling polyethylene catheter was positioned in the left ventricle of each animal via the retrograde transcarotid artery approach, with the tip passing across the aortic valve, to induced sterile vegetations. The catheter was left in place throughout the study. To determine an optimal inoculum for inducing IE, at 7 days postcatheterization the animals were infected intravenously through the tail vein with an inoculum of *S. aureus* Xen29 of 10^4, 10^5, or 10^6 CFU. Animals from all groups were shaved over the heart (ventral), as well as the kidney and spleen areas (dorsal), to optimize capture of BLS. The animals were monitored for BLS daily after infection in both the ventral and dorsal positions by using the IVIS (see below). Animals were included in the final analysis only if the catheters were correctly positioned across the aortic valve in the left ventricle at the time of sacrifice and macroscopic vegetations were visualized.

Antibiotic treatment. Infected animals were randomized to receive either (i) no therapy (untreated control), (ii) vancomycin (120 mg/kg, every 12 h [q12h], subcutaneous), (iii) cefazolin (50 mg/kg, every 8 h [q8h], intramuscular [i.m.]), or (iv) gentamicin (2.5 mg/kg, q8h, i.m.). For vancomycin therapy, potential relapse of infection was also investigated 3 days after treatment was discontinued. These antibiotic regimens were designed to achieve supra-MIC peak levels of susceptible strains in serum, based on prior data in the literature from similar models (16, 23, 24). Treatment was initiated at 3 days postinfection and administered for three consecutive days. The number of animals per group ranged from five to eight, which is based on an 80% power calculation to detect at least a twofold difference in mean tissue bacterial densities between any two groups.

Measurement of in vivo BLS. After induction of IE, animals from all groups were imaged daily using the IVIS imaging system. Total photon emissions from predefined regions of interest (ROI) of each animal were acquired daily for a maximum of 5 min (e.g., cardiac area [ventral position] and kidney and spleen areas [dorsal position]). Captured images were then quantified by using the Living Image software package (Xenogen Corp.). BLS from the ROI were expressed using a pseudocolor scale, with red representing the most intense luminescence and blue representing the least intense luminescence; the data are presented as the cumulative photon counts collected within each ROI. Uninfected animals were imaged to detect any background signals. After the final imaging time point, the animals were euthanized and target tissues (e.g., cardiac vegetations, kidneys, and spleen) were removed for both ex vivo bioluminescence imaging and quantitative cultures, as described below.

Microbiological evaluation. Untreated controls were sacrificed at 6 days after infection. Antibiotic-treated animals were sacrificed after 3-days of therapy, at least 18 h after the last antibiotic dose. As noted above, an additional group of vancomycin-treated animals was assessed for BLS for 3 days after the last vancomycin dose to identify relapsing infection. This group was then sacrificed on day 10 postinfection for target tissue quantitative culture. Animals were euthanized with 100 mg of thiopental given as a rapid bolus intraperitoneally. At sacrifice, all cardiac vegetations and kidney and spleen samples were harvested, weighed, homogenized in saline, serially diluted, and plated onto TSB agar plates for quantitative culture. Tissue homogenate cultures were grown for 24 h at 37°C, and bacterial densities were expressed as the $\log_{10}$ CFU per gram of tissue. As in previous investigations, the *S. aureus* density in target tissues ($\log_{10}$ CFU per gram of tissue) was utilized as the microbiologic end point.

Antibiotic levels in serum. Serum samples were obtained from vancomycin-treated (120 mg/kg, subcutaneous), cefazolin-treated (50 mg/kg, i.m.), or gentamicin-treated (2.5 mg/kg, i.m.) animals at 0.25, 0.5, 1, 2, 4, 6, 8, 10 and 12 h after the first dose. Antibiotic concentrations were determined by an agar diffusion well assay, by comparing zone sizes of known antibiotic concentrations with those of the rat serum samples. Vancomycin concentrations in serum were determined using *Bacillus subtilis* ATCC 6633, while cefazolin and gentamicin serum concentrations were determined using *S. aureus* RN6390. All assays were done in duplicate on samples from two or three animals. The limit of detection for these bioassays was 2 μg/ml for vancomycin and 1 μg/ml for cefazolin and gentamicin.

Statistical analysis. To statistically compare *S. aureus* tissue densities among the various groups, we used the Kruskal-Wallis test with the Tukey post hoc correction for multiple comparisons as needed. Significance was determined at $P < 0.05$. We used regression analyses to analyze the relationships between *S. aureus* densities in target tissues and BLS among the different groups ($r^2 \geq 0.5$ was considered to be significant).

RESULTS

Susceptibility testing. At an inoculum of 10^5 CFU/ml, the MICs of vancomycin, cefazolin, and gentamicin for *S. aureus* Xen29 were 0.78, 0.39, and 12.5 μg/ml, respectively. At the higher inoculum (10^7 CFU/ml), the MICs of each antibiotic were increased twofold. The MBCs of vancomycin, gentamicin, and cefazolin were the same as their respective MICs at both inocula.

In vitro BLS assays. Bioluminescent images of *S. aureus* Xen29 grown in the presence and absence of polyethylene catheters, recorded after 5 and 24 h of incubation, are shown in Fig. 2. Figure 2A and E and Fig. 2C and G show the *S. aureus* strain grown in TSBG broth with and without the catheter, respectively; Fig. 2D and H represent the BLS from the catheter after being removed from broth at 5 and 24 h of incubation, respectively. As noted, the strain grew and luminesced better in the presence of the catheter (compare Fig. 2A and C

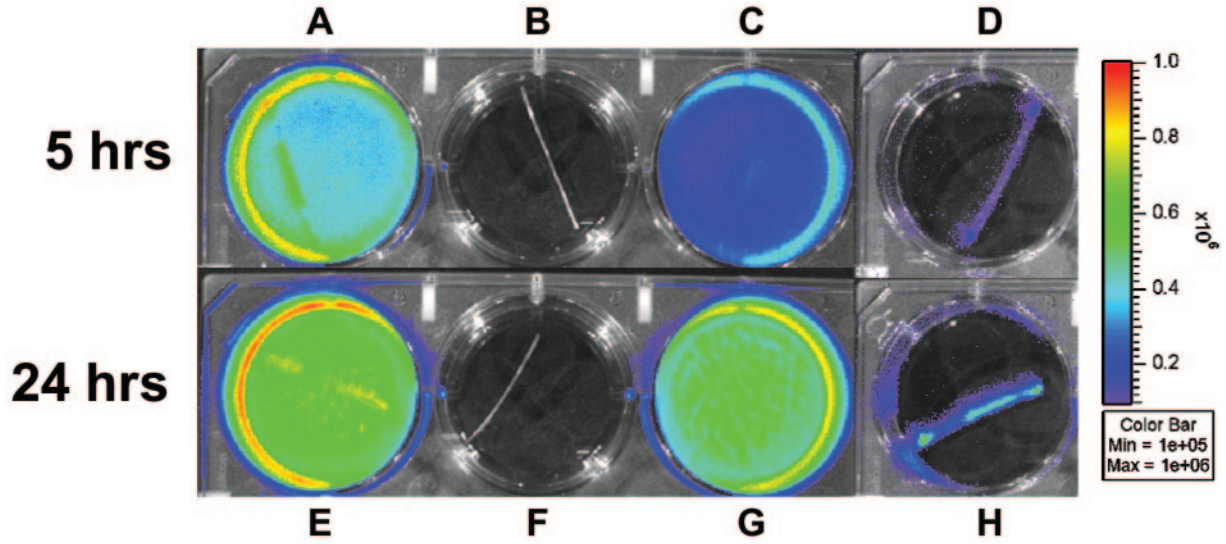

FIG. 2. Monitoring the intensity of bioluminescence of *S. aureus* Xen29 on catheter segments after 5 and 24 h of incubation at 37°C. Images were acquired with the IVIS imaging system and are displayed as pseudocolor images, with variations in color representing light intensity. (A and E) *S. aureus* Xen29 grown in TSBG with the catheter after 5 and 24 h of incubation, respectively. (C and G) *S. aureus* strain grown in TSBG without the catheter after 5 and 24 h of incubation, respectively. (D and H) BLS from the catheter after removal of TSBG, at 5 and 24 h of incubation, respectively. The lack of light signal from the control catheter (B and F) indicates the specificity of the detection system.

and compare Fig. 2E and G), especially at the 24-h time point (Fig. 2D and H). In all instances, BLS were greater at 24 h than at 5 h. No BLS were observed from catheters grown in the absence of bacteria (control; Fig. 2B and F).

Optimal inocula for inducing *S. aureus* IE in the rat model. Figure 3 shows the real-time biophotonic images of two representative rats infected with one of three different *S. aureus* inocula (10^4 to 10^6 CFU) over a 6-day postinfection period. At inocula of both 10^5 and 10^6 CFU, significant cardiac BLS were observed, demonstrating induction of IE (100% infection rate in both groups). In contrast, minimal cardiac BLS were observed from animals infected with 10^4 CFU (0% infection rate). Figure 3A and B represent a removed heart with opened left ventricle 6 days after infection with 10^5 CFU. Figure 3A shows the catheter placed in the left ventricle of the heart (small arrow) with numerous vegetations around the catheter and aortic valves (large arrows); Fig. 3B shows strong BLS from the catheter and vegetations. These observations confirmed that bioluminescence from the heart was specifically emitted from the infected catheter and vegetations. Figure 4A depicts the quantitated cardiac BLS over the postinfection period in animals infected with 10^4 to 10^6 CFU. As noted, the cardiac BLS were relatively similar in animals challenged with 10^5 or 10^6 CFU over the first 3 days of infection, with all animals exhibiting a substantial cardiac BLS. However, animals challenged with 10^6 CFU experienced 100% mortality by day 4 postinfection (Fig. 4B). The cardiac BLS in rats infected with 10^5 CFU increased and persisted in all animals over a 6-day postinfection period (Fig. 3 and 4 panel A). This latter inoculum resulted in 62% survival after 3 days of infection and 50% survival even after 6 days of infection, when the experiment was terminated (Fig. 4B). In all animals challenged with 10^4 CFU, cardiac BLS were minimal (Fig. 3 and 4A) and 100% animal survival was observed (Fig. 4B).

In vivo, no convincing BLS were detected in the areas of the kidneys or spleen at any challenge inoculum. In contrast, in ~20% of animals challenged with an inoculum of either 10^5 or 10^6 CFU, BLS were detected ex vivo in kidneys and/or spleen (data not shown). Also, no BLS were detected in catheterized animals during the preinfection observation period.

S. aureus densities in the target tissues (e.g., cardiac vegetations, kidneys, and spleen) were similar between animal groups challenged at 10^5 and 10^6 CFU (Table 1). In contrast, animals challenged with 10^4 CFU had significantly lower *S. aureus* densities in these target organs than did animals challenged at 10^5 or 10^6 CFU (Table 1). Moreover, we observed a significant positive relationship between the intensity of cardiac BLS and *S. aureus* densities in the vegetations in individual animals in the 10^5 CFU inoculum group ($r^2 = 0.75$). Therefore, based on cardiac BLS, target tissue densities, and mortality rates, 10^5 CFU was chosen as an optimal challenge dose for inducing IE with this strain and for evaluating antimicrobial strategies.

Real-time in vivo BLS detection during antibiotic therapy. Real-time in vivo cardiac bioluminescent images of representative animals from the untreated control group and from the antibiotic-treated groups are shown in Fig. 5. Each panel represents the same two animals from a given group and is compared with the cardiac BLS in untreated controls. A progressive reduction of cardiac BLS was observed in vancomycin-treated animals after the first day of treatment, and the BLS continued to decline further during therapy (Fig. 5). However, a gradual increase in BLS was seen within 2 days of discontinuing vancomycin therapy as compared to end-of-therapy images, suggesting microbiologic relapse (Fig. 5). For cefazolin, a modest decrease in cardiac BLS was observed over the 3-day therapy period (Fig. 5). In contrast, the cardiac BLS in animals treated with gentamicin showed continued increases during therapy, similar to untreated controls (Fig. 5).

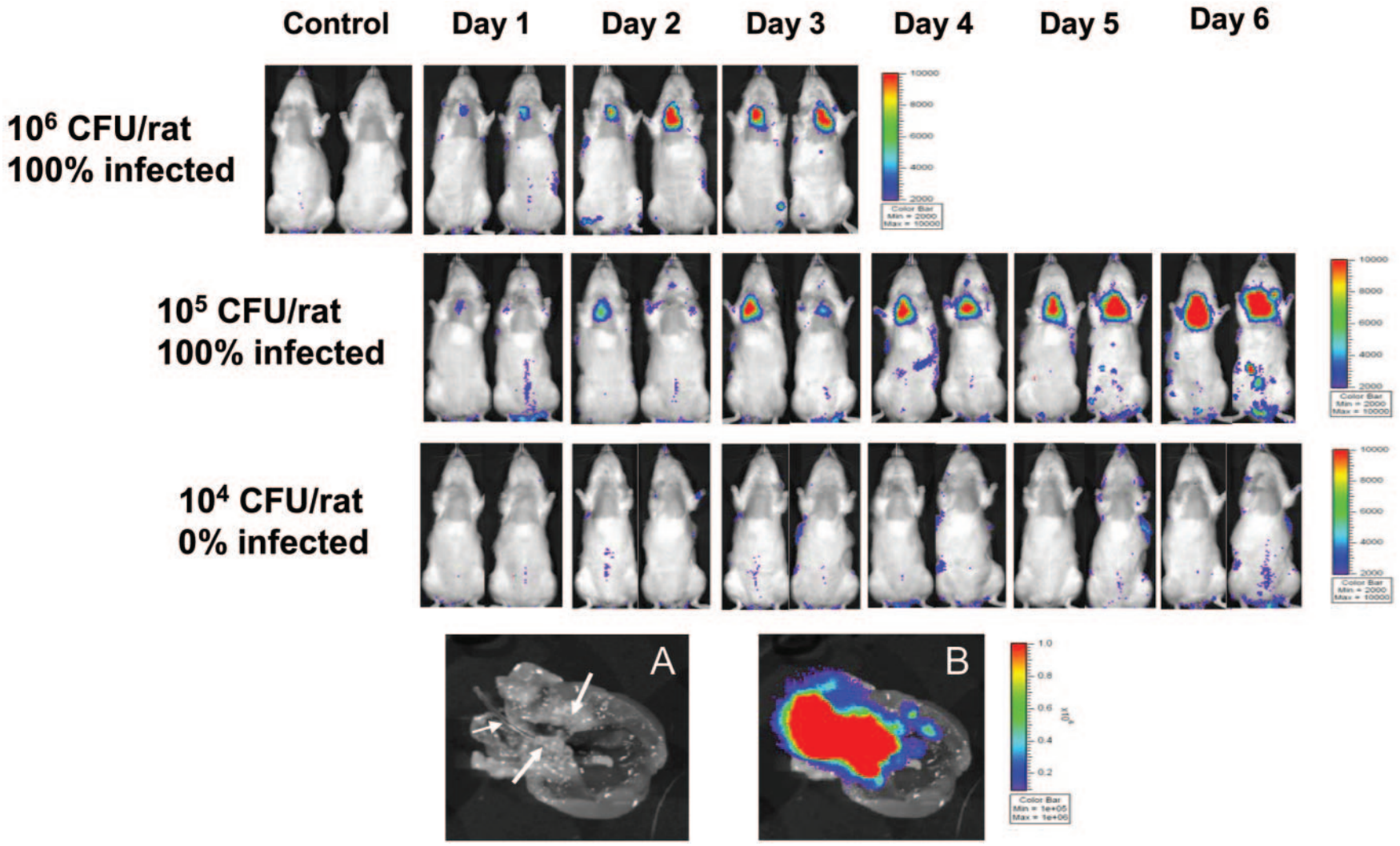

FIG. 3. Real-time monitoring of *S. aureus* Xen29 in an experimental-rat endocarditis model. Two representative animals infected intravenously with either normal saline (control) or 10^6, 10^5, or 10^4 CFU of the *S. aureus* strain are shown. The animals were imaged ventrally, with their chest area shaved, to avoid background signal from animal hair. The process of infection was monitored daily by detecting photon emission around the region of interest (heart area) over a 6-day course by using the IVIS. (A and B) Removed and opened heart from an animal infected with 10^5 CFU of *S. aureus* Xen29 after 6 days of infection. (A) The catheter is in a correct place, and numerous vegetations are visible around the aortic valves; (B) bioluminescence is emanating from the catheter and vegetations. The color bar indicates the signal intensity, with red and blue representing the high and low bioluminescent signals, respectively.

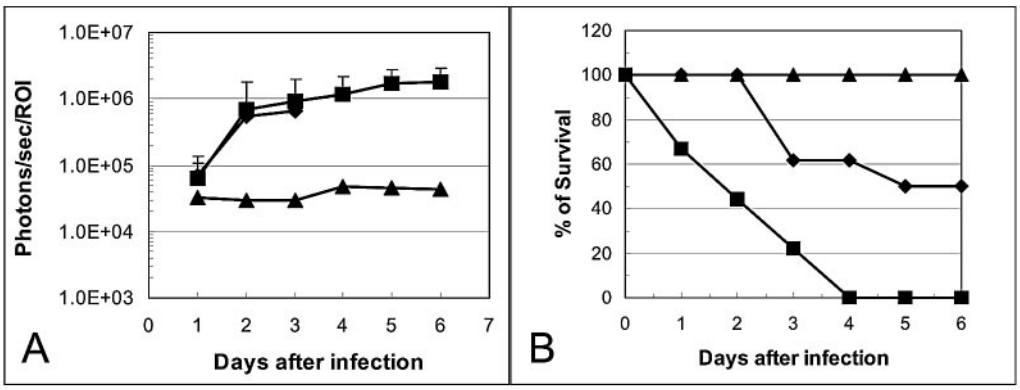

FIG. 4. (A) Bioluminescence monitoring of animals infected with 10^6 (■), 10^5 (◆), or 10^4 (▲) CFU of *S. aureus* Xen29 in the ROI in the rat endocarditis model. The total number of photons detected within the ROI was determined by using the IVIS and its computer software. Each datum point is the mean and standard error for seven to nine animals. † indicates that 100% of animals infected with 10^6 CFU of *S. aureus* Xen29 died at 4 days post-infection. Error bars indicate standard deviation. (B) Percent survival of animals infected with 10^6 (■), 10^5 (◆), or 10^4 (▲) CFU of *S. aureus* Xen29 in the rat endocarditis model.

The mean cardiac BLS for each therapy group are graphed over time in Fig. 6. Thus, the cardiac BLS from animals treated with vancomycin showed a progressive reduction compared to that from untreated controls (Fig. 6). However, bioluminescence-based evidence of a relapse was observed after discontinuation of vancomycin therapy, with increased cardiac BLS noted with respect to the vancomycin treatment period (Fig. 6). Cefazolin also caused a substantial decrease in cardiac BLS after the first day of therapy, but little change was noted thereafter during treatment (Fig. 6). For the gentamicin-treated group, the cardiac BLS profiles were very similar to those for the untreated controls (Fig. 6).

Microbiologic evaluation. *S. aureus* densities in vegetations, kidneys, and spleen in the different therapy regimens are shown in Table 2. Paralleling the BLS data discussed above, treatment with vancomycin resulted in significant decreases in *S. aureus* densities in all three target tissues (~2 to 3 $\log_{10}$ CFU/g of tissue; $P < 0.005$) compared to untreated controls. Also, as predicted by BLS profiles, evidence of a microbiologic relapse was observed after discontinuation of vancomycin therapy, with higher *S. aureus* densities seen in all three target tissues than those at the end of the vancomycin therapy. Cefazolin treatment caused a ~1.0-$\log_{10}$ CFU/g reduction in vegetation densities ($P < 0.05$ versus the control), consistent with the modest decreases observed in cardiac BLS. Gentamicin therapy caused no substantive reductions in *S. aureus* vegetation densities, paralleling the persistently high cardiac BLS (Table 2).

TABLE 1. *S. aureus* density in cardiac vegetations, kidneys, and spleen with different inocula in the rat endocarditis model

Inoculum (no. of animals)	Mean $\log_{10}$ CFU/g of tissue ± SD[a] in:		
	Vegetation	Kidney	Spleen
10^6CFU/animal(9)	10.36 ± 0.85	7.30 ± 0.64	6.70 ± 0.57
10^5CFU/animal(8)	9.93 ± 0.53	7.14 ± 0.53	6.44 ± 0.63
10^4CFU/animal(7)	3.46 ± 0.50*	1.81 ± 0.74*	1.58 ± 0.59*

[a] SD, standard deviation. * $P < 0.001$ with respect to 10^5 or 10^6 CFU-challenged animals.

Relationship between cardiac BLS and *S. arueus* densities in vegetations. A comparison of mean cardiac BLS intensities and the mean staphylococcal vegetation densities was carried out by regression analyses for untreated controls, vancomycin-treated groups, vancomycin relapse groups, cefazolin-treated groups, and gentamicin-treated groups. A significant correlation was noted between the mean cardiac BLS intensity and mean *S. aureus* densities in vegetations among untreated controls and antibiotic-treated animals ($r^2 = 0.68$).

Antibiotic levels in serum. The peak concentrations of vancomycin (subcutaneously) and cefazolin (i.m.) in serum were reached after 4 and 2 h postdose, respectively, with achievable peak concentrations at >10× the MIC of both agents against the infecting strain at these time points (data not shown). Of note, the time above MIC was substantially longer for vancomycin (>12 h) than for cefazolin (~4 h), paralleling the better microbiologic and BLS efficacies of vancomycin in this model. Gentamicin mean peak concentrations in serum (~4 μg/ml) were below the MIC of the drug for this strain.

DISCUSSION

In recent years there has been a dramatic increase in the number of antibiotic-resistant strains of *S. aureus* (e.g., methicillin-resistant and vancomycin-intermediate *S. aureus*) causing life-threatening infections in humans (1–3, 8, 14, 19, 22). Conventional methods for monitoring these pathogens in experimental-animal models not only are cumbersome but also usually include microbiologic assessment strategies that represent late or end stages of the disease process. These technologies require sacrifice of animals and removal of tissue. Therefore, there are no internal controls within a given animal, raising potential confounding variables due to animal-to-animal variability. In addition, these in vivo assays may be influenced by variations in tissue sampling techniques. Moreover, such studies are often expensive and labor-intensive.

A number of recent studies have emphasized the advantages of in vivo bioluminescent imaging for real-time monitoring of bacterial infections and their treatment (4, 5, 7, 9–11, 13, 21),

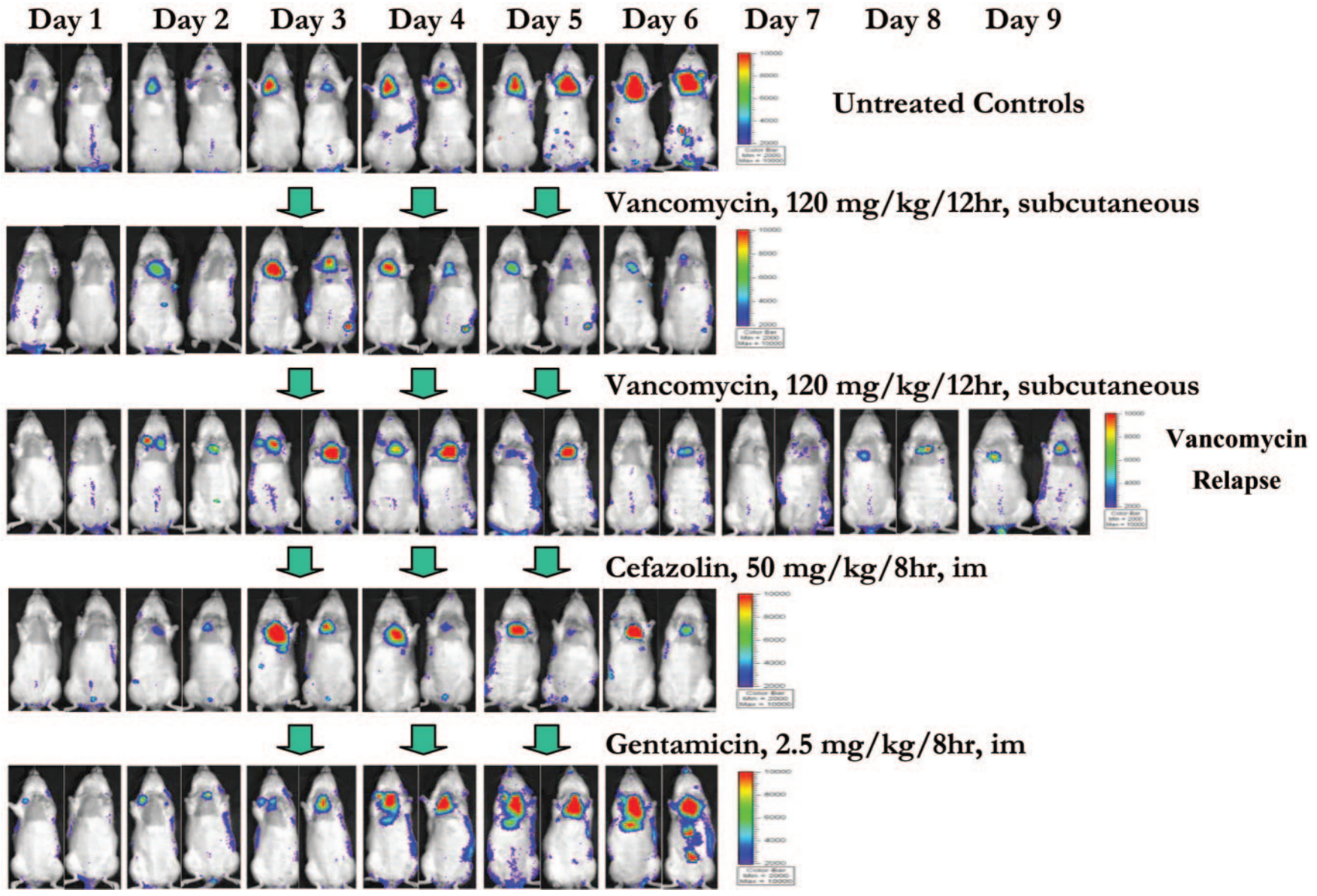

FIG. 5. Real-time monitoring of the efficacy of vancomycin, cefazolin, and gentamicin in the experimental rat model of endocarditis due to *S. aureus* Xen29. Two representative animals from the untreated control and the antibiotic-treated groups are shown. Three days after infection with 10^5 CFU of *S. aureus* Xen29, the animals received either no antibiotics (untreated control), vancomycin (120 mg/kg every 12 h, subcutaneous), cefazolin (50 mg/kg every 8 h, i.m.), or gentamicin (2.5 mg/kg every 8 h, i.m.) for 3 days. Vancomycin relapse was studied 3 days after discontinuation of the treatment. The photon signals from all groups were monitored daily after infection by using the IVIS. The color bar indicates the signal intensity, with red and blue representing high and low bioluminescence, respectively.

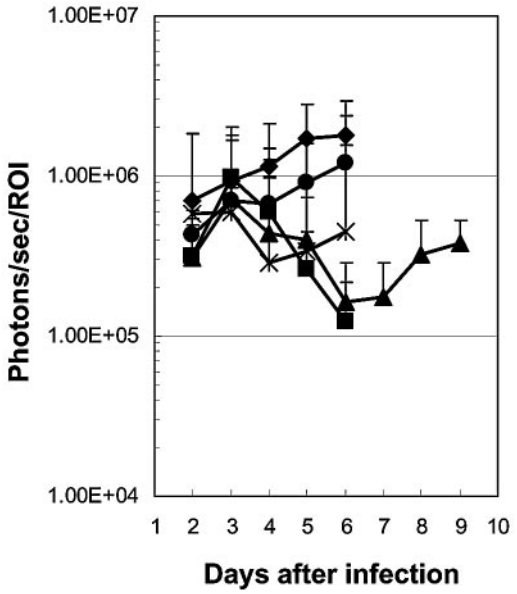

FIG. 6. Bioluminescence monitoring of the efficacy of vancomycin, cefazolin, or gentamicin in the rat *S. aureus* Xen29 endocarditis model. The total number of photons within the cardiac ROI was determined for all groups by using the IVIS. Each datum point indicates the mean and standard deviation for five to eight animals. Symbols: ◆, untreated control; ■, vancomycin; ▲, vancomycin relapse; X, cefazolin; ●, gentamicin.

showing it to be significantly more sensitive, rapid, and noninvasive than standard techniques. In addition, this technology allows quantitative numeric data to be obtained spatially from defined areas of the animal. Importantly, in vivo bioluminescent imaging enables each animal to be used as its own control over time without the need for sequential sacrifices at relevant time points, thus mitigating the problem of animal-to-animal variations. This latter ability not only significantly improves biostatistics through collection of multiple data points in the same animal but also helps to minimize the use of experimental animals. Further, once a correlation between photon emission and CFU for a given pathogen in a given target tissue is established, the bioluminescence intensities can be used to monitor the metabolic status and bacterial burden at specific sites of infection in vivo without animal sacrifice.

In the present studies, we used an *S. aureus* strain (ATCC 12600) which was bioluminescently engineered (Xen29) by using the gram-positive *lux* operon delivery transposon, Tn*4001 luxABCDE* (9–11). Using this constitutively bioluminescent strain, we were able to see both spatial and sequential information pertaining to the progression of the infection in vivo. Previous studies by Kadurugamuwa et al. have demonstrated the use of this bacterial strain and bioluminescent imaging techniques to monitor subcutaneous, catheter-associated *S. aureus* infection in mice and have shown that the efficacies of selected antimicrobial agents against such infections could be rapidly evaluated in vivo in real time (9, 10). In addition, they used this technology to predict in vivo development of rifampin resistance during therapy (11).

TABLE 2. *S. aureus* density in target tissues with antibiotic treatment in the rat endocarditis model

Group (no. of animals)	Mean $\log_{10}$ CFU/g of tissue ± SD[a] in:		
	Vegetation	Kidney	Spleen
Untreated control (8)	9.93 ± 0.53	7.14 ± 0.53	6.44 ± 0.63
Vancomycin (6)	6.03 ± 1.30**	3.84 ± 1.32**	4.26 ± 0.92**
Vancomycin relapse (5)	8.27 ± 0.65	5.23 ± 0.94*	5.50 ± 0.83
Cefazolin (5)	8.80 ± 0.97*	5.12 ± 1.40*	4.39 ± 0.97*
Gentamicin (5)	9.41 ± 0.53	5.37 ± 0.58**	5.14 ± 0.65*

[a] SD, standard deviation. * $P < 0.05$ with respect to control; ** $P < 0.005$ with respect to control.

To date, bioluminescent imaging has not been utilized to monitor the progression or therapy of experimental endovascular infections. Therefore, in the present study, we adapted this system to the rat IE model and evaluated the therapeutic efficacy of several antibiotics in real time. Several interesting observations emerged from this investigation. In untreated control animals infected with a 10^5 CFU challenge, there was a significant correlation between the quantitative *S. aureus* burden in cardiac vegetations and the intensity of the bioluminescent signals from the heart. These data are consistent with findings by other investigators using the catheter-induced soft-tissue infection model (7, 9–11, 13, 21). In addition, the microbiologic efficacy of several conventional antistaphylococcal agents (as measured by reductions in cardiac vegetation bacterial densities) was mirrored by real-time changes in the intensity of cardiac bioluminescence. Thus, for this vancomycin- and cefazolin-susceptible *S. aureus* strain, treatment with each agent resulted in significant reductions in cardiac vegetation bacterial densities (vancomycin > cefazolin), paralleling the relative reductions in the intensity of the cardiac BLS. These overall microbiologic and cardiac BLS differences were attributable at least in part to the better pharmacokinetic and pharmacodynamic profile of vancomycin than that of cefazolin at dose strategies used in this study. It should be emphasized that the IVIS system accurately identified these differences in real time. Of note, gentamicin therapy of this gentamicin-resistant strain had in little impact on vegetation bacterial densities and cardiac bioluminescent intensities. Moreover, microbiologic relapse following discontinuation of vancomycin therapy was accurately predicted by observing increased bioluminescence. Importantly, regression analyses revealed a significant correlation between mean vegetation bacterial densities and mean BLS intensities in both untreated controls and antibiotic-treated animals.

It is interesting that no photon signals were detected over the kidneys or spleen in vivo and that only a minority of such target organs emitted photon signals ex vivo, despite *S. aureus* counts of >6 $\log_{10}$CFU/g of tissue in these two target organs. There are several conceivable explanations for this apparent paradox in the IE model. For example, a threshold tissue bacterial density may be required for photon image detection, since *S. aureus* densities are significantly higher in vegetations than in the kidneys and spleen in this model, by ~2 $\log_{10}$ CFU/g of tissue (Tables 1 and 2). In addition, the tissue distribution of hematogenous staphylococcal infection in the kidneys and spleen tends to be more diffuse than observed within cardiac vegetations, potentially mitigating the overall photon intensity (12). Furthermore, the anatomic distance between the camera and the cardiac catheter may be shorter than that

between the camera and the kidneys or spleen, anatomically blunting the photon signal. Also, since the infecting strain grew and luminesced maximally in the presence of the catheter, its absence in such metastatic foci may also reduce the photon signal. Other potential factors that may have mitigated the BLS from the kidneys and spleen compared to that from cardiac vegetations include (i) distinct microenvironmental characteristics of these anatomic niches, including low pH and high white cell influxes in abscesses, compared to cardiac vegetations and (ii) interference by hemoglobin of the photon signal in these organs (20). Investigations are in progress to study this phenomenon further.

As with any study, the use of a single staphylococcal strain may limit the generalizability of our conclusions. However, similar results have been obtained using the current strain in a different model of *S. aureus* infection (9). Moreover, similar data emerged when a distinct bioluminescent *S. aureus* strain (8325-4) was used (7, 13).

In conclusion, our results demonstrate that the experimental-rat IE model is readily adaptable to real-time monitoring of endovascular infections by bioluminescent imaging. In addition to evaluating antibiotic efficacy, this model should prove to be a useful tool in determining bacterial virulence gene expression profiles in vivo. Since the half-life of the bioluminescent signal is very short (1 to 2 h), this technology overcomes the limitations of other gene reporter systems (e.g., green fluorescent protein), in which signals with long half-lives signals complicate the capacity to define "on-off" profiles of genes of interest (26, 27).

ACKNOWLEDGMENTS

This work was supported in part by grants from the American Heart Association 0265054Y (to Y.Q.X.) and the National Institutes of Health AI-39108 (to A.S.B.).

We thank Yin Li for excellent technical assistance.

REFERENCES

1. **Archer, G. L.** 1998. *Staphylococcus aureus:* a well-armed pathogen. Clin. Infect. Dis. **26:**1179–1181.
2. **Bayer, A. S., and W. M. Scheld.** 1999. Endocarditis and intravascular infections, p. 857–902. *In* G. L. Mandell, J. E. Bennett, and R. F. Dolin (ed.), Principles and practices of infectious diseases. Churchill-Livingstone, Inc., New York, N.Y.
3. **Bayer, A. S., A. F. Bolger, K. A. Taubert, W. Wilson, J. Stockelberg, A. W. Karchmer, et al.** 1998. Diagnosis and management of infective endocarditis and its complications. Circulation **98:**2936–2948.
4. **Contag, C. H., P. R. Contag, I. Mullins, S. D. Spilman, D. K. Stevenson, and D. A. Benaron.** 1995. Photonic detection of bacterial pathogens in living host. Mol. Microbiol. **18:**593–603.
5. **Contag, P. R., I. N. Olomu, D. K. Stevenson, and C. H. Contag.** 1998. Bioluminescent indicators in living mammals. Nat. Med. **4:**245–247.
6. **Entenza, J. M., J. Vouillamoz, M. P. Glauser, and P. Moreillon.** 1999. Efficacy of trovaflozacin in treatment of experimental staphylococcal or streptococcal endocarditis. Antimicrob. Agents Chemother. **43:**77–84.
7. **Francis, K. P., D. Joh, C. Bellinger-Kawahara, M. J. Hawkinson, T. F. Purchio, and P. R. Contag.** 2000. Monitoring bioluminescent *Staphylococcus aureus* infections in living mice using a novel *luxABCDE* construct. Infect. Immune. **68:**3594–3600.
8. **Herwaldt, L. A.** 1999. Control of methicillin-resistant *Staphylococcus aureus* in the hospital setting. Am. J. Med. **106:**11S–18S.
9. **Kadurugamuwa, J. L., L. V. Sin, J. Yu, K. P. Francis, R. Kimura, T. Purchio, and P. R. Contag.** 2003. Rapid direct method for monitoring antibiotics in a mouse model of bacterial biofilm infection. Antimicrob. Agents Chemother. **47:**3130–3137.
10. **Kadurugamuwa, J. L., L. Sin, E. Albert, J. Yu, K. P. Francis, M. DeBer, M. Rubin, C. Bellinger-Kawahare, T. R. Parr, Jr., and P. R. Contag.** 2003. Direct continuous method for monitoring biofilm infection in a mouse model. Infect. Immun. **71:**882–890.
11. **Kadruugamuwa, J. L., L. V. Sin, J. Yu, K. P. Francis, T. Purchio and P. R. Contag.** 2004. A non-invasive optical imaging method to evaluate post-antibiotic effects on biofilm infection in vivo. Antimicrob. Agents Chemother. **48:**2283–2287.
12. **Krause, J. R., and S. P. Levison.** 1976. Pathology of infective endocarditis, p. 55–86. *In* D. Kaye (ed.), Infective endocarditis. University Park Press, Baltimore, Md.
13. **Kuklin, N. A., G. D. Pancari, T. W. Tobery, L. Cope, J. Jackson, C. Gill, K. Overbye, K. P. Francis, J. Yu, D. Montgomery, A. S. Anderson, W. McClements, and K. U. Jansen.** 2003. Real-time monitoring of bacterial infection in vivo: development of bioluminescent staphylococcal foreign-body and deep-thigh-wound mouse infection models. Antimicrob. Agents Chemother. **47:**2740–2748.
14. **Lowy, F. D.** 1998. *Staphylococcus aureus* infections. N. Engl. J. Med. **339:** 520–532.
15. **Moreillon, P., J. M. Entenza, P. Francioli, D. McDevitt, T. J. Foster, P. Francois, and P. Vaudaux.** 1995. Role of *Staphylococcus aureus* coagulase and clumping factor in pathogenesis of experimental endocarditis. Infect. Immun. **63:**4738–4743.
16. **Murphy, T. M., J. M. Deitz, P. J. Petersen, S. M. Mikels, and W. J. Weiss.** 2000. Therapeutic efficacy of GAR-936, a novel glycylcycline, in a rat model of experimental endocarditis. Antimicrob. Agents Chemother. **44:** 3022–3027.
17. **National Committee for Clinical Laboratory Standards.** 2000. Antimicrobial susceptibility test for bacteria that grow aerobically. Approved standard, 5th ed. NCCLS document M7-A5. National Committee for Clinical Laboratory Standards, Wayne, Pa.
18. **National Committee for Clinical Laboratory Standards.** 1999. Methods for determining bactericidal activity of antimicrobial agents. Approved guideline. NCCLS document M26-A. National Committee for Clinical Laboratory Standards, Wayne, Pa.
19. **Projan, S. J.** 2000. Antibiotic resistance in the staphylococci, p. 463–470. *In* V. A. Fischetti, R. P. Novick, J. J. Ferretti, D. A. Portnoy, and J. I. Rood (ed). Gram-positive pathogens. ASM Press. Washington, D.C.
20. **Rice, B. W., M. D. Cable, and M. B. Nelson.** 2001. In vivo imaging of light-emitting probes. J. Biomed. Optics **6:**432–440.
21. **Rocchetta, H. L., C. J. Boylan, J. W. Foley, P. W. Iversen, D. L. LeTourneau, C. L. McMillian, P. R. Contag, D. E. Jenkins, and T. R. Parr, Jr.** 2001. Validation of a noninvasive, real-time imaging technology using bioluminescent *Escherichia coli* in the neutropenic mouse thigh model of infection. Antimicrob. Agents Chemother. **45:**129–137.
22. **Sieradzki, K., R. B. Roberts, S. W. Haber, and A. Tomasz.** 1990. The development of vancomycin resistance in a patient with methicillin-resistant *Staphylococcus aureus* infection. N. Engl. J. Med. **340:**517–523.
23. **Steckelberg, J. M., M. S. Rouse, B. M. Tallan, D. R. Osmon, N. K. Henry, and W. R. Wilson.** 1993. Relative efficacies of broad-spectrum cephalosporins for treatment of methicillin-susceptible *Staphylococcus aureus* experimental infective endocarditis. Antimicrob. Agents Chemother. **37:**554–558.
24. **Voorn, G. P., J. Thompson, W. H. F. Goessens, W. Schmal-Bauer, P. H. M. Broeders, and M. F. Michel.** 1991. Role of tolerance in cloxacillin treatment of experimental *Staphylococcus aureus* endocarditis. J. Infect. Dis. **163:**640–643.
25. **Xiong, Y. Q., L. I. Kupferwasser, P. M. Zack, and A. S. Bayer.** 1999. comparative efficacies of liposomal amikacin (Mikasome) plus oxacillin versus conventional amikacin plus oxacillin in experimental endocarditis induced by *Staphylococcus aureus:* microbiological and echocardiographic analyses. Antimicrob. Agents Chemother. **43:**1737–1742.
26. **Xiong, Y. Q., A. S. Bayer, M. R. Yeaman, W. van Wamel, A. C. Manna, and A. L. Cheung.** 2004. Impacts of *sarA* and *agr* in *Staphylococcus aureus* strain Newman on fibronectin-binding protein A gene expression and fibronectin adherence capacity in vitro and in experimental infective endocarditis. Infect. Immun. **72:**1832–1836.
27. **Xiong, Y. Q., W. van Wamel, C. C. Nast, M. R. Yeaman, A. L. Cheung, and A. S. Bayer.** 2002. Activation and transcriptional interaction between *agr* RNAII and RNAIII in *Staphylococcus aureus in vitro* and in an experimental endocarditis model. J. Infect. Dis. **186:**668–677.